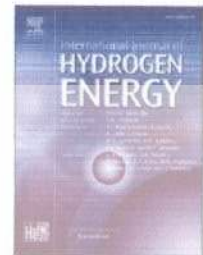
Available online at [www.sciencedirect.com](http://www.sciencedirect.com)

ScienceDirect

journal homepage: [www.elsevier.com/locate/he](http://www.elsevier.com/locate/he)

## A new method for optimal parameters identification of a PEMFC using an improved version of Monarch Butterfly Optimization Algorithm

Songjian Bao<sup>a</sup>, Abdolghaffar Ebadi<sup>b</sup>, Mohsen Toughani<sup>c</sup>,  
Juhriyansyah Dalle<sup>d</sup>, Andino Maselena<sup>e</sup>, Baharuddin<sup>f</sup>,  
Abdullah Yıldızbası<sup>g,\*</sup>

<sup>a</sup> Department of Electronic Engineering, School of Electronic Information and Electrical Engineering, Chongqing University of Arts and Sciences, Chongqing, 402160, China

<sup>b</sup> Department of Agriculture, Jouybar Branch, Islamic Azad University, Jouybar, Iran

<sup>c</sup> Department of Fishery, Islamic Azad University Babol Branch, Babol, Iran

<sup>d</sup> Department of Information Technology, Universitas Lambung Mangkurat, Banjarmasin, 70123, Indonesia

<sup>e</sup> STMIK Pringsewu, Lampung, Indonesia

<sup>f</sup> Department of Electrical Engineering Education, Universitas Negeri Medan, North Sumatera, Indonesia

<sup>g</sup> Department of Industrial Engineering, Ankara Yıldırım Beyazıt University (AYBU), 06010, Ankara, Turkey

### HIGHLIGHTS

- A new technique proposed for optimal selection of PEMFC parameters
- The method is based on a new model of Coyote Optimization Algorithm
- The achieved results showed a good confirmation by the experimental data

### ARTICLE INFO

#### Article history:

Received 19 January 2020

Received in revised form

1 April 2020

Accepted 28 April 2020

Available online xxx

#### Keywords:

Parameter identification

Proton exchange membrane fuel

Monarch Butterfly Optimization

Improved

### ABSTRACT

In this paper, a circuit-based model of proton exchange membrane fuel cell (PEMFC) is developed for optimal selection of the model parameters. The optimization is based on using an improved version of Monarch Butterfly Optimization (IMBO) algorithm for minimizing the Integral Time Absolute Error between the measured output voltage and the output voltage of the achieved model. For validation of the proposed method, two different case studies including 6 kW NedSstack PS6 and 2 kW Nexa FC PEMFC stacks have been employed and the results have been compared with the experimental data and some well-known metaheuristics including Chaotic Grasshopper Optimization Algorithm (CGOA), Grass Fibrous Root Optimization Algorithm (GRA), and basic Monarch Butterfly Optimization (MBO) to indicate the superiority of the proposed method against the compared methods. Final results show a satisfying agreement between the proposed IMBO and the experimental data.

\* Corresponding author.

E-mail address: [yildizbasi.abdullah@gmail.com](mailto:yildizbasi.abdullah@gmail.com) (A. Yıldızbası).

<https://doi.org/10.1016/j.ijhydene.2020.04.256>

0360-3199/© 2020 Hydrogen Energy Publications LLC. Published by Elsevier Ltd. All rights reserved.



Circuit-based model  
Integral time absolute error

© 2020 Hydrogen Energy Publications LLC. Published by Elsevier Ltd. All rights reserved.

## Introduction

A set of different factors such as fossil resource constraints, negative environmental impacts, hydrocarbon utilization, rising fossil fuel prices, political conflicts and its effects on sustainable energy supply force the policy makers and experts to move towards the creation of a new technology with higher security of energy supply, environmental protective, and higher energy system efficiency [1–3]. Accordingly, hydrogen is one of the best options to play as a safe alternative in this new energy delivery system. Hydrogen as the most abundant element on Earth is produced in various ways. The provided electricity from renewable sources such as wind, solar, and geothermal can be used for hydrogen generation [4–6]. The generated hydrogen is then saved and transferred to the locations to be used in a variety of applications, including small electronics, transportation industry, and power plants. However, many people believe that the ultimate fuel for the human society is hydrogen and that human will be experienced the hydrogen era in a not too distant future. Some prominent features of the hydrogen that distinguish it from other fuel options are its abundance, almost unique consumption, negligible emission of pollutants, reversibility of its production cycle, and reduced greenhouse effects. Hydrogen power system due to independence from primary energy sources, is a permanent, sustainable, immovable, inclusive and renewable system and it is predicted that in the near future, its production and consumption as energy carrier will spread throughout the world economy and stabilize the hydrogen economy. However, one should not expect hydrogen to compete with other energy carriers in terms of cost of production at the beginning step, in the future hydrogen will play a central role in controlling urban pollution. The conversion of chemical energy in hydrogen into electrical energy is carried out by fuel cells. Fuel cells have great potential as one of the future energy sources in hybrid systems due to their many advantages and rapid advancement in their technology [7,8]. Hydrogen, after being extracted from hydrocarbon or water sources, is considered as a sustainable fuel in energy sources by fuel cells. Nowadays, due to the expansion of wind and solar power sources in different countries and the availability of high and low-cost energy, the possibility of hydrogen extraction from the electrolysis process of water has become economical [9]. Therefore, the use of fuel cells in hybrid systems as one of the sources of energy conversion and generation along with solar and wind energy sources is a serious option. A more popular type among fuel cells is proton-exchange membrane fuel cell (PEMFC) [10]. PEMFC are high-efficiency power generators that can achieve 40%–50% electrical efficiency at different power scales. The basis of energy production in PEMFCs is the exothermic reaction between hydrogen and oxygen present in the air. The

result of this reaction is electricity, heat and distilled water. The benefits of PEMFCs such as lighter weight, solid electrolyte, short start-up time without noise, variability, and the ability to renew the system in a closed cycle independent of the battery have attracted research into replacing the polymer fuel cell system with satellite batteries [11,12].

Generally, mathematical modeling of the PEMFCs is an important category that can be used for optimal designing the system [13,14]. This modeling is based on considering physical and electrochemical processes to govern the fuel cell efficiency [15–18]. The model includes a differential equation system along with its determined constraints to define the transition processes and their relations. Based on the explained cases and due to the importance of the PEMFC modeling, several researchers have been worked on this subject [19].

Rahman et al. [20] presented both modeling and empirical results for a PEMFC operating based on its open circuit voltage to restricting current conditions. The results were verified by limiting current tests and polarization curves based on different operation conditions. Simulations showed that the proposed 1-D dry model has a good agreement with experimental results.

Yang et al. [21] employed an adaptive neuro-fuzzy inference system (ANFIS) for modeling a 250 W PEMFC that is placed on an electric bicycle. To determine the system configuration, humidity, temperature, hydrogen, oxygen flowrate, and current were adopted as the inputs and the efficiency and the voltage were considered as the outputs of the ANFIS. Simulation results showed that using ANFIS for modeling the PEMFC gives a reliable and accurate result to predict the PEMFC performance. However, the classic methods and the ANN gave logical results, by introducing the metaheuristics, the researchers were attracted to use these types of solvers to resolve the modeling problem with a simple and time saving procedure. For example, Yang et al. [21] proposed a hybrid neural network and metaheuristic for parameter estimation of a proton exchange membrane fuel cell (PEMFC). They used a new hybrid optimization algorithm, called hybrid world cup optimization (WCO) and fluid Search Optimization (FSO) algorithm to optimize the efficiency of an improved version of Elman neural network. The method was also verified based on four different operational conditions. Simulation results were compared with some well-known metaheuristics and the results showed higher efficiency with good agreement with the experimental data of the PEMFC.

Yin and Razmjoo [22] proposed another optimal method based on deer hunting optimization (DHO) algorithm to estimate the PEMFC parameters. The DHO algorithm has been adopted to improve PEMFC parameters identification. The method was then verified based on different operational conditions and the results were compared with different



algorithms. Final results indicated the superiority of the method in achieving the PEMFC model parameters.

Cao et al. [15] presented another optimized model for parameter identification of the PEMFCs. The main objective was to propose a developed model of seagull optimization algorithm to optimal selection of the PEMFC stack parameters. Two experimental-based data including BCS 500-W and NedStack PS6 were used for algorithm verification and the results were compared with some different optimization algorithms to show the method's higher efficiency.

This study presents a new developed metaheuristic technique with desirable search ability with the ability of making good trade-off between exploration and exploitation search for optimal selection of the PEMFC stack model parameters, i.e. the proposed developed algorithm improves the basic algorithm in terms of diversity and balance of exploitation and exploration. The algorithm also attempts to resolve the basic algorithm premature convergence shortcoming. The total contributions of the algorithm are briefly given below:

- Designing a new improved metaheuristic for parameter estimation of PEMFC.
- The method is based on a new model of Monarch Butterfly Optimization Algorithm.
- The method is verified by two empirical data, NedStack PS6 and Nexa FC.
- The final configuration is compared with empirical data and some well-known algorithms.

The rest of the paper is organized as follows: **Dynamic mechanism of model of proton exchange membrane fuel cell** discusses about the model of the PEMFC, in **Monarch Butterfly Optimization algorithm**, the improved version of Monarch Butterfly Optimization as one contribution of this paper is briefly explained. **Simulation results** illustrates the simulation results of the proposed method on two experimental case studies and the paper is concluded in **Conclusion**.

## Dynamic mechanism of model of proton exchange membrane fuel cell

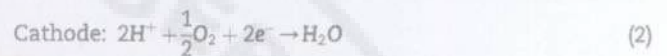
### PEMFC modeling

PEMFCs consist of a series of electrode membranes including electrodes, electrolytes and catalysts, and gas diffusion layers. A layer of catalyst, carbon, and electrode is sprayed onto the solid electrolyte and a carbon sheet is pressed on each side to protect the cell and act as the electrode [23]. The most basic part of the triple phase boundary cell (TPB) is where the electrolyte, the catalyst, and the reactants are fused together or where the cell's primary reaction occurs. The important point is that the membrane should not be electrically conductive so that half the reactions are not mixed. A fuel cell with a polymer membrane converts the chemical energy released during the electrochemical reaction of hydrogen and oxygen into electrical energy, in contrast to the direct combustion process of hydrogen and oxygen gases that generate thermal energy. The hydrogen gas enters the fuel cell from the anode side. At the anode and adjacent to the catalyst it

becomes a proton and an electron. Hydrogen oxidation is expressed as follows:



The proton penetrates the cathode through the electrolytic membrane. The electrons also move to the cathode through the outer charge circuit, which generates the electrical current of the fuel cell output. In the meantime, a stream of oxygen enters the fuel cell through the cathode, forming a chemical reaction with water molecules in combination with protons transported from the anode and electrons through the outer orbit. This oxygen resuscitation reaction is formulated below:



And the overall reaction is as follows:



The reverse reaction is expressed in the above equations, showing the re-fusion of the protons of hydrogen and electron together with the oxygen molecule and the production of the water molecule. Fig (1) shows a basic structure of a PEMFC.

To provide a basic perception about PEMFC for analyzing its output parameters including current density and output voltage, the mathematical model has been required. The output voltage of a PEMFC stack can be formulated as follows.

$$V_{FC} = E_{\text{Nerst}} - V_{\text{act}} - V_{\text{con}} - V_{\Omega} \quad (4)$$

where,  $V_{\Omega}$  represents the ohmic overpotential voltage,  $V_{\text{con}}$  describes the concentration overpotential,  $V_{\text{act}}$  determines the activation overvoltage, and  $E_{\text{Nerst}}$  represents the Nernst potential and is obtained as following:

$$E_{\text{Nerst}} = V^{\circ} - k_{\text{F}} T_{\text{FC}} - \lambda_{\text{e}} I(s) \frac{\tau_{\text{e}} S}{\tau_{\text{e}} S + 1} + \frac{RT}{2F} \left( \ln p_{\text{H}_2} + \frac{1}{2} \ln p_{\text{O}_2} \right) \quad (5)$$

where,  $V^{\circ}$  represents the reference voltage,  $T_{\text{FC}}$  determines the temperature of fuel cell ( $^{\circ}\text{C}$ ),  $\lambda_{\text{e}}$  is a constant factor ( $\Omega$ ),  $F$  stands for the Faraday constant,  $k_{\text{F}}$  represents the empirical constant ( $\text{V/K}$ ), and  $p_{\text{O}_2}$  and  $p_{\text{H}_2}$  determine the oxygen and hydrogen partial pressures (Pa). Fig. (2), shows a circuit model of the output voltage for PEMFC.

If  $n$  cells accumulated with a fuel cell system, the voltage  $V_{\text{out}}$  is achieved as follows:

$$V_{\text{T}} = N \times V_{\text{FC}} \quad (6)$$

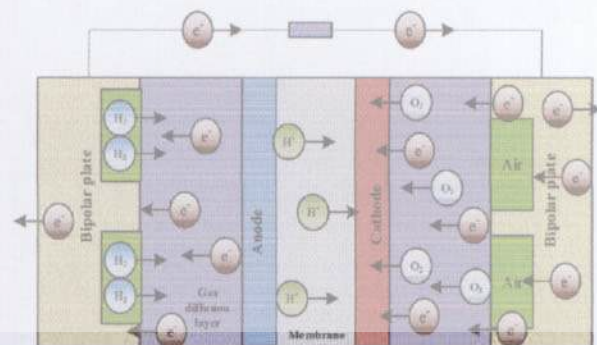


Fig. 1 – The basic structure of a PEMFC.



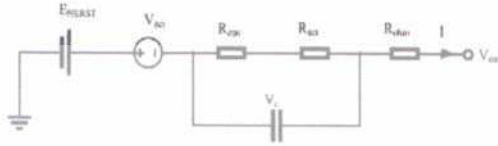


Fig. 2 – The circuit-model of a PEMFC.

Based on literature review, there are some research works with determinative differences between the membrane-electrode connection voltage levels of identical fuel cells at the same conditions that makes  $V^*$  as a parameter that should be selected optimally [24].  $\tau_e$  and  $\lambda_e$  are two other parameters in model that should be optimally selected. Another part of model that needs optimization for its unknown parameters is ohmic resistance. Based on the electrical modeling from Fig. (2), this term can be achieved by the following equation:

$$R_{ohm} = R_m + R_t \quad (7)$$

where,  $R_t$  stands for the equivalent resistance for the transferred protons through the membrane, and  $R_m$  represents the membrane resistance that is achieved as follows [25]:

$$R_m = \frac{181.6 \times l \times \left[ 1 + 0.03 \times \frac{l}{A} + 0.062 \times \left( \frac{T_{FC}}{303} \right)^2 \times \left( \frac{l}{A} \right)^{2.5} \right]}{A \times \left( \phi - 0.634 - \frac{3l}{A} \right) \times e^{\left( \frac{4.18 \times T_{FC} - 30}{T_{FC}} \right)}} \quad (8)$$

where,  $l$  describes the fuel cell thickness, and  $\phi$  represents an adjustable parameter that depends to the relative humidity, the membrane age, and the anode gas stoichiometric ratio. Here,  $l$  and  $\phi$  are also considered as two unknown parameters that should be optimized.

Also, the mass transport losses decrease the concentration of the reactant on the surface of electrodes. This term can be formulated as follows [26].

$$R_{con} = B \times I^{-1} \times \ln \left( \frac{I_{mr}}{I_{mr} - I} \right) \quad (9)$$

where,  $B$  represents an experimentally value which depends to the operation state of the cell, and  $I_{mr}$  describes the maximum current ratio of the electrode and is obtained by the following Eq. (26).

$$I_{mr} = D \times N_r \times F \times C_b \times \tau^{-1} \quad (10)$$

where,  $D$  describes the reacting effective diffusion,  $N_r$  represents the number of electrons that are adopted for the reaction,  $C_b$  determines the bulk concentration, and  $\tau$  stands for the thickness of the diffusion layer.

From Fig. (2), model contains a capacitor to simulate the effect of double-layer charging between the membrane and porous cathode. This voltage is obtained by the following equation:

$$V_c = \left( I - C \frac{dV_c}{dt} \right) \times (R_{con} + R_{act}) \quad (11)$$

Since the capacitance parameter ( $C$ ) has some

uncertainties due to the porous behavior of PEMFC, this term has been assumed as an unknown parameter for optimization.

Another term of the model based on Fig. (2) is the activation loss that decreases the speed of the reactions on the surface of electrode. This term is mathematically formulated as follows:

$$V_{act} = \xi_1 + \xi_2 \times T + \xi_3 \times T_{FC} \times \ln(CO_2) + \xi_4 \times T_{FC} \times \ln(I) \quad (12)$$

where,  $\xi_i$  points to pseudo-experimental values, and  $CO_2$  defines the oxygen concentration at the cathode/gas interface ( $\text{mol.cm}^{-3}$ ) and is achieved as follows:

$$CO_2 = pO_2 \times 5.08 \times 10^8 \times e^{-498T - 1} \quad (13)$$

And  $CH_2$  defines the Hydrogen concentration at the anode membrane/gas interface ( $\text{mol.cm}^{-3}$ ) as follows:

$$CH_2 = p_{H_2} \times \left[ 10.9 \times 10^7 \times e^{\left( \frac{-1}{T} \right)} \right]^{-1} \quad (14)$$

The main parameter values for the PEMFC model are given in Table 1 [24,27,28].

#### PEMFC model parameters optimization

For optimal selection of the aforementioned unknown parameters, a new optimization algorithm has been employed. The purpose of this algorithm is to minimize the Integral of Absolute Error (IAE) value between the optimized model voltage and the actual voltage that is extracted from experimental data. The IAE minimization as an objective function is given in the following equation:

$$\min \sum_{i=1}^m |V_{FC}^i - V_{ident}^i| \quad (15)$$

where,  $m$  stands for the number of empirical data for training, and  $V_{FC}$  and  $V_{ident}$  describe the actual and the estimated voltages for the PEMFC stack, respectively. Eq. (15) will be performed subject to the following constraints (Table 2):

As can be observed, due to using interval constraints instead of algebraic equations, classic optimization methods fail to achieve the global minimum of this problem. This reason made us to design a metaheuristic-based optimization algorithm to solve the optimal parameter identification problem of the PEMFC stack model.

In recent years, the application of metaheuristic-based methods for solving parameter identification is exponentially increasing [29–33]. Metaheuristic-based methods often have been inspired by different nature phenomena. For

Table 1 – The main parameter values for the PEMFC model [24,27,28].

| Parameter   | Value  | Unit        |
|-------------|--------|-------------|
| $V^*$       | 1.229  | V           |
| $\lambda_e$ | 3.3    | $\Omega$    |
| $\tau_e$    | 80     | s           |
| $F$         | 96.487 | kC/mol      |
| $R_t$       | 300    | $\mu\Omega$ |
| $\phi$      | <23    | –           |



**Table 2 – The required limitations for the unknown parameters for optimization.**

| Parameter      | Minimum value | Maximum value        | Unit            |
|----------------|---------------|----------------------|-----------------|
| C              | 0.1           | 10                   | F               |
| A              | 90            | 130                  | cm <sup>2</sup> |
| B              | 0.01          | 0.1                  | V               |
| l              | 51            | 89                   | m               |
| λ <sub>0</sub> | 0             | 0.01                 | Ω               |
| V*             | 0.1           | 2                    | V               |
| φ              | 1             | 23                   | –               |
| ξ <sub>1</sub> | 0             | 1                    | –               |
| ξ <sub>3</sub> | 0             | 1 × 10 <sup>-4</sup> | –               |
| ξ <sub>4</sub> | 0             | 1 × 10 <sup>-3</sup> | –               |

And, ξ<sub>2</sub> = 0.003 + 0.0002 ln(A) + 43 × 10<sup>-6</sup> ln(C<sub>fit</sub>).

instance, Emperor Penguin Optimizer (EPO) inspired based on the swarm living of emperor penguins, Coyote Optimization Algorithm (COA) [42] inspired by coyotes survival behavior in the nature, Deer Hunting Optimization Algorithm (DHOA) [43] inspired based on how to hunt the deer.

Among different aforementioned metaheuristics, one of the newest efficient algorithms is Monarch Butterfly Optimization (MBO) that is introduced by Wang et al., in 2019. This algorithm simulates the unique behavior of the monarch butterflies as the only species which migrate to the tropical zones like birds. The main purpose of this paper is to improve this algorithm's efficiency by applying some new mechanisms for PEMFC parameter identification.

### Monarch Butterfly Optimization algorithm

#### Basic Monarch Butterfly Optimization (MBO) algorithm

Monarch Butterfly Optimization (MBO) Algorithm starts with a random and uniform population that is called monarch butterflies population. This population includes the solution candidates of the problem. MBO divides the population into two groups: Land 1 and Land 2. Therefore, the number of monarch butterfly individuals in subpopulation Land 1 and Land 2 are as follows:

$$\text{Land 1} = NP_1 \times \text{ceil}(p \times NP) \tag{16}$$

$$\text{Land 2} = NP - NP_1 \times (NP_2) \tag{17}$$

where, NP describes the total number of populations, ceil(x) rounds x to the nearest integer greater than or equal to x, and p determines the monarch butterflies' ratio in Land 1. The new child population in the algorithm is generated by the monarch butterfly parents of both Lands. In the event that the parent has better value than the generated child, to keep the population number constant, it has been replaced with the child. This keeps efficient patents for the next generation. This conception can be formulated as follows:

$$x_{i,k}^{t+1} = x_{r_1,k}^t \tag{18}$$

where, x<sub>i,k</sub><sup>t+1</sup> describes the kth element of position (x<sub>i</sub>) of monarch butterfly i at generation t+1, x<sub>r<sub>1</sub>,k</sub><sup>t</sup> defines the kth updated

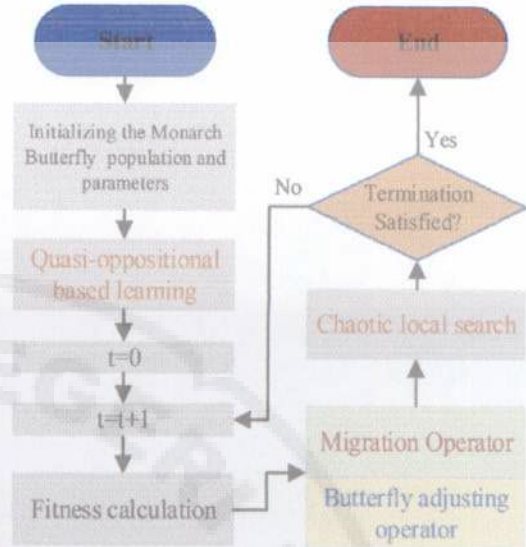


**Fig. 3 – The flowchart diagram of the proposed IMBO.**

element of x<sub>r<sub>1</sub></sub> for the individual r<sub>1</sub>, and t represents the number of current iterations. The individual r<sub>1</sub> is randomly selected from Land 1. If r has less value than or equal to p, r is achieved by the following equation:

$$r = \rho \times \tau \tag{19}$$

where, τ describes the period of migration, and ρ defines a uniform and random number. In contrast, if the p has a value less than r, the element k for the new butterfly is achieved by the following:

$$x_{i,k}^{t+1} = x_{r_2,k}^t \tag{20}$$

where, x<sub>r<sub>2</sub>,k</sub><sup>t</sup> describes the kth updated element of x<sub>r<sub>1</sub></sub> for the individual r<sub>1</sub> that is obtained randomly from the Land 2. An interesting advantage of the algorithm is in making a logical trade-off between Land 1 and Land 2 such that when p has bigger value, a large number of populations is selected from Land 1, otherwise, most of population will be selected from Land 2. If the generated child for the monarch butterfly i has smaller value than or equal to p, the position has been updated as follows:

$$x_{i,k}^{t+1} = x_{Best,k}^t \tag{21}$$

where, x<sub>Best,k</sub><sup>t</sup> describes the kth individual of x<sub>Best</sub> that gives the best result in the population.

If p has a value less than ρ, the position has been updated as follows:

$$x_{i,k}^{t+1} = x_{r_3,k}^t \tag{22}$$

$$r_3 \in [1, 2, \dots, NP_2] \tag{23}$$

where, x<sub>r<sub>3</sub>,k</sub><sup>t</sup> describes the kth randomly selected member of x<sub>r<sub>3</sub></sub> from Land 2.

During the algorithm, if the rate of butterfly adjustment (R<sub>ba</sub>) is less than ρ, the position has been updated as follows:

$$x_{i,k}^{t+1} = x_{i,k}^t + \alpha \times (dx_k - 0.5) \tag{24}$$



where,  $dx$  represents the walk step of the individual  $i$  and is achieved as follows:

$$dx = \text{Levy}(x_i^k) \quad (25)$$

where,  $\alpha$  points to the weighting coefficient, such that:

$$\alpha = \frac{sm}{t^2} \quad (26)$$

where,  $sm$  represents the maximum walk step that is passed by a butterfly in one step.

By considering a big value for  $\alpha$ , a long search step has been resulted that increases the impact of  $dx$  on  $x_{j,k}^{t+1}$  applied to the exploration term. In other hand, if  $\alpha$  has small value, short search step will be made for  $x_{j,k}^{t+1}$  and will result and exploitation mechanism.

### Improved monarch butterfly optimization (IMBO) algorithm

Based on aforementioned explanations, excessive exploration of MBO algorithm during high value of  $\alpha$  gives an incompetent time-consuming result after some iterations. For resolving this problem, two different mechanisms have been employed that are explained in the following.

#### Quasi-oppositional based learning

To understand the conception of Quasi-oppositional mechanism, the oppositional-based learning should be first explained. The oppositional-based learning is a term for improving the precision and the convergence speed by comparing of the considered candidate with its opposite and selecting the best one as the new candidate [34,35]. For better illustration of the opposite number, consider  $NP$  as a real number in a  $D$ -dimensional search space limited in the interval  $[L, U]$ . The opposite of the candidate  $NP$  is defined by  $\widehat{NP}$  and is achieved by the following:

$$\widehat{NP}_i = L_i + U_i - NP_i \quad (27)$$

$$i = 1, 2, \dots, D \quad (28)$$

By considering the definition of opposite number, the quasi-opposite number is defined by  $\widehat{NP}$  as follows [36]:

$$\widehat{NP}_i = \text{rand} \left( \frac{U_i + L_i}{2}, NP_i \right) \quad (29)$$

This mechanism can be briefly explained by the following pseudo-code:

#### Chaotic local search

The present study also uses chaotic local search for more modification. This mechanism can be used for resolving the

```

for i=1:N
  for j=1:D
    OX(i,j)=l(j)+u(j)-np(i,j);
    c(j)=(l(j)+u(j))/2;
    if OX(i,j)<c(j)
      QOX(i,j)=c(j)+(OX(i,j)-c(j))*rand;
    else
      QOX(i,j)=OX(i,j)+(c(j)-OX(i,j))*rand;
    end
  end
end
end

```

Table 3 – The utilized functions for the verification.

| Formulation  | Range               | F*     |
|--|---------------------|--------|
| $F1 = x \times \sin(4x) + 1.1y \times \sin(2y)$                                | $0 < x, y < 0$      | -18.55 |
| $F2 = 0.5 + \frac{\sin^2(\sqrt{x^2 + y^2} - 0.5)}{1 + 0.1(x^2 + y^2)}$         | $0 < x, y < 2$      | 0.5    |
| $F3 =  x  +  y  + (x^2 + y^2)^{0.25} \times \sin(30((x + 0.5)^2 + y^2)^{0.1})$ | $[-\infty, \infty]$ | -0.25  |
| $F4 = 10n + \sum_{i=1}^n (x_i^2 - 10 \cos(2\pi x_i))$ , $n = 9$                | $[-5.12, 5.12]$     | 0      |

algorithm premature convergence [37,38]. A typical form of chaos theory is as follows:

$$CM_{l+1}^n = f(CM_l^n) \quad (30)$$

Where,  $l = 1, 2, \dots, n$ ,  $n$  describes the dimension map and  $f(CM_l^n)$  represents the chaotic model.

The present study uses a well-known chaotic mechanism, called logistic map for modification. By applying logistic map to the population,

$$\gamma_{n+1} = \omega \times \gamma_n \times (1 - \gamma_n) \quad (31)$$

where,  $\omega = 4$ , and  $\gamma_n$  represents the value of the chaotic mechanism in iteration  $n$  in the range  $[0, 1]$  [37,38]. Accordingly, the chaotic sequence,  $\sigma_{o,n,q}$ , is formulated as follows:

$$\sigma_{o,n,q} = 4 \times \gamma_{o,n,q} \times (1 - \gamma_{o,n,q}) \quad (32)$$

where,  $o$  represents the system generators quantity,  $n$  describes the population number, and  $q$  stands for the iteration number.

By adopting Eq. (31) as the chaotic mechanism for the monarch butterfly individuals,

$$x_{i,k}^{t+1} = x_{i,k}^t + \sigma_{o,n,q} \times (dx_k - 0.5) \quad (33)$$

Fig. (3) shows the diagram flowchart of the proposed IMBO algorithm.

To validate the proposed IMBO, it has been applied to four test functions and the results have been compared with some well-known algorithms. The compared algorithms include Chaotic grasshopper optimization algorithm for global optimization (CGOA) [39], Grass Fibrous Root Optimization Algorithm (GRA) [40], and basic Monarch Butterfly Optimization (MBO) [41] to show its prominence. Table 3 indicates the details of the test functions.

Based on this study, the algorithm will be stopped when the maximum number of evaluated functions are achieved. Table 4 indicates the validation results of the compared algorithms by considering the four defined test functions. The



**Table 4 – The validation results of the compared algorithms.**

|    |            | CGOA [39] | GRA [40] | MBO [41] | IMBO   |
|----|------------|-----------|----------|----------|--------|
| F1 | Maximum    | -9.85     | -11.27   | -11.20   | -10.35 |
|    | Minimum    | -18.45    | -18.50   | -18.48   | -18.53 |
|    | Median std | -15.48    | -16.05   | -16.36   | -16.54 |
|    |            | 4.75      | 2.31     | 3.26     | 2.64   |
| F2 | Maximum    | 0.534     | 0.542    | 0.511    | 0.503  |
|    | Minimum    | 0.500     | 0.500    | 0.500    | 0.500  |
|    | Median std | 0.536     | 0.542    | 0.570    | 0.563  |
|    |            | 0.025     | 0.003    | 0.001    | 0.000  |
| F3 | Maximum    | -0.064    | -0.143   | -0.223   | -0.237 |
|    | Minimum    | -0.245    | -0.249   | -0.253   | -0.256 |
|    | Median std | -0.125    | -0.176   | -0.230   | -0.241 |
|    |            | 0.143     | 0.204    | 0.014    | 0.011  |
| F4 | Maximum    | 17.36     | 22.43    | 7.25     | 1.19   |
|    | Minimum    | 2.016     | 0.005    | 0.000    | 0.000  |
|    | Median std | 7.391     | 9.470    | 0.464    | 0.095  |
|    |            | 4.186     | 6.954    | 0.329    | 0.076  |

validation is based on evaluating Median value, standard deviation (std) value, minimum, and the maximum values of the objective function.

Fig. (4) shows the convergence profile of the compared algorithms during the validation on the test functions. From the results, it is obvious that the proposed IMBO algorithm has the best accuracy among different compared algorithms. The

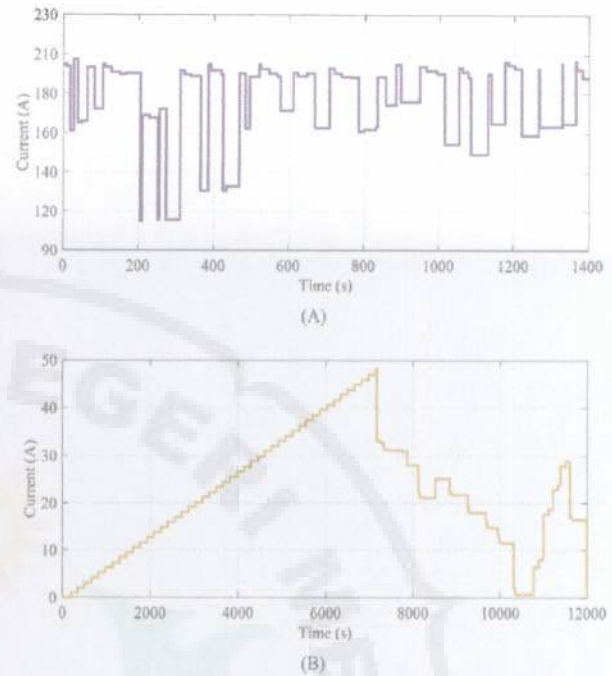


**Fig. 5 – The current profile adopted by (A) NedStack PS6 and (B) 2 kW Nexa for validation.**

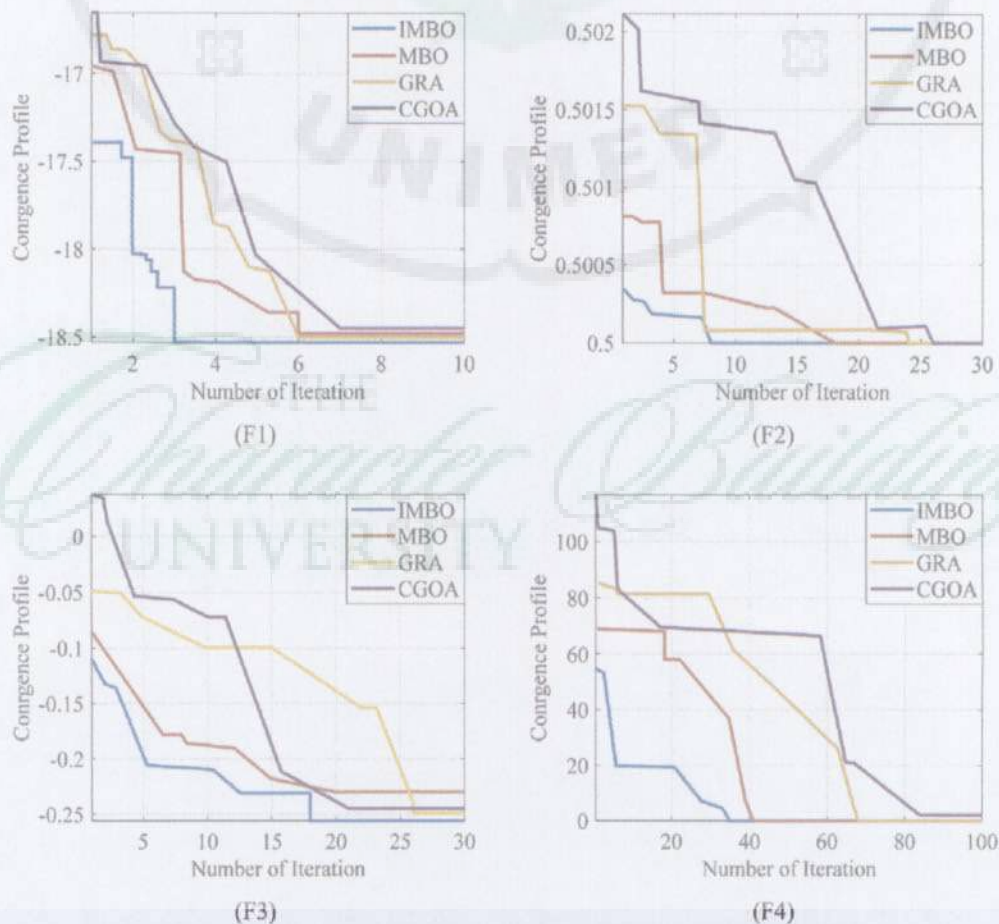


**Fig. 4 – The convergence profile of the compared algorithms.**



Table 5 – The validation results of the proposed IMBO algorithm compared with other well-known algorithms for NedSstack PS6 PEMFC.

| Parameter   | Method                 |                        |                        |                        | Unit            |
|-------------|------------------------|------------------------|------------------------|------------------------|-----------------|
|             | IMBO                   | MBO [41]               | GRA [40]               | CGOA [39]              |                 |
| $E_0^0$     | 1.29                   | 1.42                   | 1.20                   | 1.32                   | V               |
| $\xi_1$     | -1.92                  | -0.897                 | -1.16                  | -1.03                  | -               |
| $\xi_2$     | $1.98 \times 10^{-3}$  | $2.31 \times 10^{-3}$  | $1.75 \times 10^{-3}$  | $1.75 \times 10^{-3}$  | -               |
| $\xi_3$     | $7.92 \times 10^{-5}$  | $7.62 \times 10^{-5}$  | $5.93 \times 10^{-5}$  | $7.84 \times 10^{-5}$  | -               |
| $\xi_4$     | $-9.54 \times 10^{-4}$ | $-9.37 \times 10^{-4}$ | $-9.29 \times 10^{-4}$ | $-9.48 \times 10^{-4}$ | -               |
| A           | 211.37                 | 237.20                 | 209.15                 | 210.58                 | cm <sup>2</sup> |
| $\phi$      | 15.80                  | 16.18                  | 14.53                  | 15.93                  | -               |
| $\lambda_e$ | 0.010                  | 0.008                  | 0.004                  | 0.01                   | $\Omega$        |
| l           | $13.25 \times 10^{-6}$ | $15.82 \times 10^{-6}$ | $13.40 \times 10^{-6}$ | $12 \times 10^{-6}$    | m               |
| B           | 0.054                  | 0.048                  | 0.039                  | 0.072                  | V               |
| C           | 5.57                   | 5.80                   | 4.93                   | 5.17                   | F               |

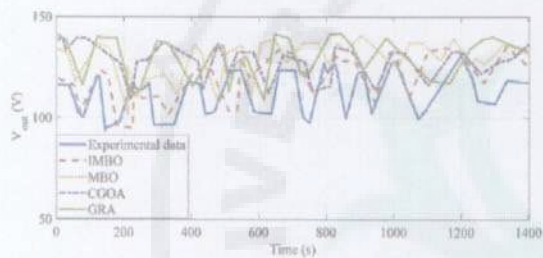


Fig. 6 – The results of different algorithms for NedSstack PS6 parameter identification based on voltage profile.

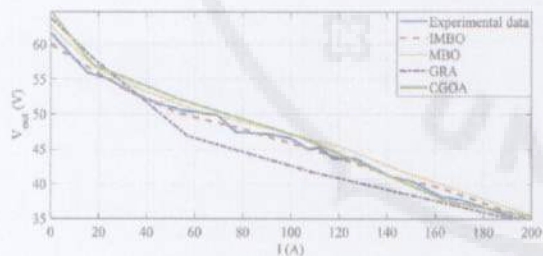


Fig. 7 – The results of different algorithms for NedSstack PS6 parameter identification based on voltage-current profile.

minimum value of the IMBO also shows its higher robustness toward the others.

### Simulation results

In this study, two standard benchmarks including 6 kW NedSstack PS6 PEMFC and 2 kW Nexa PEMFC have been adopted for validation the proposed algorithm. Fig. (5) shows the current profile for training the PEMFC models in 6 kW NedSstack PS6 PEMFC (A) and 2 kW Nexa PEMFC (B), respectively.

The system simulation and programming are performed by MATLAB R2017b. The required parameters for the proposed IMBO for optimal parameters selection of the PEMFC are:  $N_P = 50$ ,  $N_c = 10$  with 100 iterations. Based on the mentioned assumptions, the results for the two analyzed case studies are given in the following.

#### 6 kW NedSstack PS6 PEMFC

The first case study is based on the information collected by the available data sheet of NedStack PS6 fuel cell, 6 kW [42]. In this case study, the number of cells are considered 65. Each cell contains an area of 240 cm<sup>2</sup> with 178  $\mu$ m thickness. The cell temperature is 343 K and the range of supply pressure is in the

Table 6 – The validation results of the proposed IMBO algorithm compared with other well-known algorithms for Nexa PEMFC.

| Parameter   | Method                  |                         |                         |                        | Unit            |
|-------------|-------------------------|-------------------------|-------------------------|------------------------|-----------------|
|             | IMBO                    | MBO [41]                | GRA [40]                | CGOA [39]              |                 |
| $V^*$       | 1.324                   | 1.286                   | 1.319                   | 1.320                  | V               |
| $\xi_1$     | -0.356                  | -0.428                  | -0.376                  | -1.030                 | -               |
| $\xi_3$     | $6.471 \times 10^{-5}$  | $5.736 \times 10^{-5}$  | $6.137 \times 10^{-5}$  | $7.480 \times 10^{-5}$ | -               |
| $\xi_4$     | $-9.153 \times 10^{-4}$ | $-1.682 \times 10^{-4}$ | $-1.443 \times 10^{-4}$ | $-9.48 \times 10^{-4}$ | -               |
| A           | 119.35                  | 116.50                  | 116.76                  | 210.58                 | cm <sup>2</sup> |
| $\phi$      | 15.76                   | 14.69                   | 14.08                   | 15.930                 | -               |
| $\lambda_e$ | 0.015                   | 0.008                   | 0.005                   | 0.010                  | $\Omega$        |
| l           | $19 \times 10^{-6}$     | $47 \times 10^{-6}$     | $43 \times 10^{-6}$     | $12 \times 10^{-6}$    | m               |
| B           | 0.077                   | 0.051                   | 0.064                   | 0.072                  | V               |
| C           | 5.24                    | 6.37                    | 5.96                    | 5.170                  | F               |



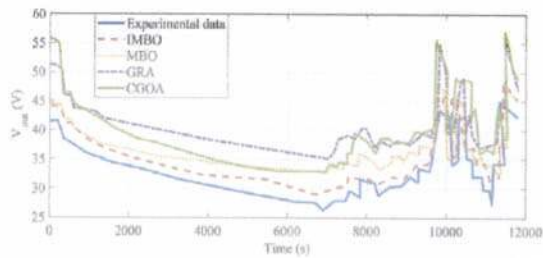


Fig. 8 – The results of different algorithms for Nexa PEMFC parameter identification based on voltage profile.

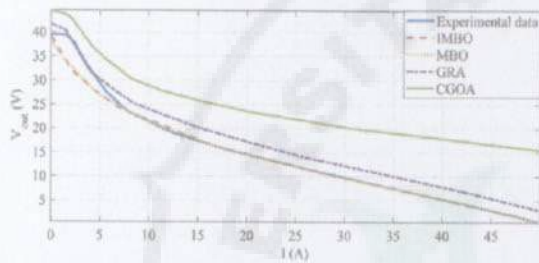


Fig. 9 – The results of different algorithms for Nexa PEMFC parameter identification based on voltage-current profile.

range [0.5, 5] bar. The output voltage of NedSstack is limited between 32 V and 60 V DC, and the range of operation is in the range [0, 225] A. Table 5 indicates the validation results of the proposed IMBO algorithm compared with other well-known algorithms including GRA [40], CGOA [39], and MBO [41] for optimal selection of the NedSstack PS6 PEMFC parameters. The results show the mean value for 30 independent runs.

Fig. (6) shows the output voltage profile for the experimental data, the proposed IMBO algorithm and the other compared algorithms. As can be observed, the proposed IMBO

algorithm has the most agreement to the experimental compared with other analyzed algorithms.

Fig. (7) shows the voltage-current profile of the experimental and estimated results for NedSstack PEMFC based on the proposed algorithm and the compared algorithms. As can be observed from Fig. (7), the estimated model based on the proposed IMBO has the best agreement with the experimental profile which shows its prominence than the other compared methods for this case study.

#### The 2 kW nexa PEMFC

The next case study is to verify the algorithms by the information collected by the available data sheet of 2 kW Nexa PEMFC [43]. Table 6 illustrates the validation results of the proposed IMBO algorithm compared with other well-known algorithms including GRA [40], CGOA [39], and MBO [41] for optimal selection of the 2 kW Nexa PEMFC parameters.

Fig. (8) and Fig. (9) show the voltage and the voltage-current profiles of different algorithms for the Nexa PEMFC parameter identification based on voltage profile. The validation is based on the load profile of the experimental data compared with proposed IMBO and some well-known methods including GRA [40], CGOA [39], and basic MBO [41].

It is observed that the proposed IMBO has the maximum agreement to the experimental data for optimal PEMFC modeling. Fig. (10) shows the value of the Integral Time Absolute Error (ITAE) for the proposed IMBO compared with GRA [40], CGOA [39], and basic MBO [41]. Fig. (10) shows that the presented IMBO algorithm has the minimum value of ITAE for both case studies.

#### Conclusions

This study proposed a new procedure for optimal parameter selection of proton exchange membrane fuel cell (PEMFC). The procedure is based on using a new improved version of

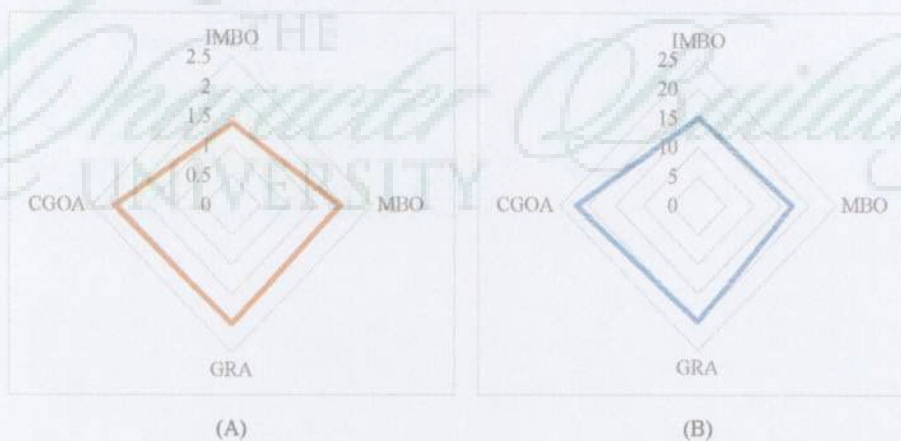


Fig. 10 – The radar plot of ITAE for minimum value for (A) NedSstack PEMFC and (B) Nexa PEMFC.



Monarch Butterfly Optimization (MBO) for minimizing the Integral Time Absolute Error (ITAE) between the experimental data and the optimal achieved model. The system analysis was based on a circuit-based model of the PEMFC and parameters contain data from 2 kW Nexa PEMFC and 6 kW NedSstack PS6 PEMFC. The simulations applied based on MATLAB software and the results of the proposed IMBO were compared with some well-known algorithms including GRA, CGOA, and basic MBO to show the prominence of the presented algorithm.

## Acknowledgement

The project is supported by open project fund of Chongqing University new energy storage device and Application Engineering Research Center - Research on SAW Pressure Sensor (No. KF20180204).

## REFERENCES

- [1] Aghajani G, Ghadimi N. Multi-objective energy management in a micro-grid. *Energy Rep* 2018;4:218–25.
- [2] Liu Y, Wang W, Ghadimi N. Electricity load forecasting by an improved forecast engine for building level consumers. *Energy* 2017;139:18–30.
- [3] Gollou AR, Ghadimi N. A new feature selection and hybrid forecast engine for day-ahead price forecasting of electricity markets. *J Intell Fuzzy Syst* 2017;32(6):4031–45.
- [4] Mirzapour F, Lakzaei M, Varamini G, Teimourian M, Ghadimi N. A new prediction model of battery and wind-solar output in hybrid power system. *J Ambient Int Hum Com* 2019;10(1):77–87.
- [5] Hosseini Firouz M, Ghadimi N. Optimal preventive maintenance policy for electric power distribution systems based on the fuzzy AHP methods. *Complexity* 2016;21(6):70–88.
- [6] Hamian M, Darvishan A, Hosseinzadeh M, Lariche Mj, Ghadimi N, Nouri A. A framework to expedite joint energy-reserve payment cost minimization using a custom-designed method based on Mixed Integer Genetic Algorithm. *Eng Appl Artif Intell* 2018;72:203–12.
- [7] Leng H, Li X, Zhu J, Tang H, Zhang Z, Ghadimi N. A new wind power prediction method based on ridgelet transforms, hybrid feature selection and closed-loop forecasting. *Adv Eng Inf* 2018;36:20–30.
- [8] Akbary P, Chiasi M, Pourkheranjani MRR, Alipour H, Ghadimi N. Extracting appropriate nodal marginal prices for all types of committed reserve. *Comput Econ* 2019;53(1):1–26.
- [9] Ebrahimian H, Barmayoon S, Mohammadi M, Ghadimi N. The price prediction for the energy market based on a new method. *Economic research-Ekonomska istraživanja* 2018;31(1):313–37.
- [10] Chugh S, Chaudhari C, Sonkar K, Sharma A, Kapur G, Ramakumar S. Experimental and modelling studies of low temperature PEMFC performance. *Int J Hydrogen Energy* Mar 2020;45(15):8866–74.
- [11] Chevalier S, Trichet D, Auvity B, Olivier J, Josset C, Machmoum M. Multiphysics DC and AC models of a PEMFC for the detection of degraded cell parameters. *Int J Hydrogen Energy* 2013;38(26):11609–18.
- [12] Rasheed RKA, Liao Q, Caizhi Z, Chan SH. A review on modelling of high temperature proton exchange membrane fuel cells (HT-PEMFCs). *Int J Hydrogen Energy* 2017;42(5):3142–65.
- [13] Fei X, Xuejun R, Razmjooy N. Optimal configuration and energy management for combined solar chimney, solid oxide electrolysis, and fuel cell: a case study in Iran. *Energy Sources, Part A Recovery, Util Environ Eff* 2019;1–21.
- [14] Yuan Z, Wang W, Wang H, Razmjooy N. A new technique for optimal estimation of the circuit-based PEMFCs using developed Sunflower Optimization Algorithm. *Energy Rep* 2020;6:662–71.
- [15] Cao Y, Li Y, Zhang G, Jermisittiparsert K, Razmjooy N. Experimental modeling of PEM fuel cells using a new improved seagull optimization algorithm. *Energy Rep* 2019;5:1616–25.
- [16] Cao Y, Wu Y, Fu L, Jermisittiparsert K, Razmjooy N. Multi-objective optimization of a PEMFC based CCHP system by meta-heuristics. *Energy Rep* 2019;5:1551–9.
- [17] Eslami Mahdiyeh, et al. A new formulation to reduce the number of variables and constraints to expedite SCUC in bulky power systems. *Proc Natl Acad Sci India Sect A (Phys Sci)* 2019;89(2):311–21.
- [18] Saeedi Mohammadhossein, et al. Robust optimization based optimal chiller loading under cooling demand uncertainty. *Appl Therm Eng* 2019;148:1081–91.
- [19] Reddy KJ, Sudhakar N. A new RBFN based MPPT controller for grid-connected PEMFC system with high step-up three-phase IBC. *Int J Hydrogen Energy* 2018;43(37):17835–48.
- [20] Rahman MA, Mojica F, Sarker M, Chuang P-YA. Development of 1-D multiphysics PEMFC model with dry limiting current experimental validation. *Electrochim Acta* 2019;320:134601.
- [21] Yang D, Pan R, Wang Y, Chen Z. Modeling and control of PEMFC air supply system based on TS fuzzy theory and predictive control. *Energy* 2019;188:116078.
- [22] Yin Z, Razmjooy N. Pemfc identification using deep learning developed BY improved deer hunting optimization algorithm. *Int J Power Energy Syst* 2020;40(2).
- [23] Larminie J, Dicks A, McDonald MS. Fuel cell systems explained. Chichester, UK: J. Wiley; 2003.
- [24] Shakhshir SA, Gao X, Berning T. An experimental study of the effect of a turbulence grid on the stack performance of an air-cooled proton exchange membrane fuel cell. *J Electrochemical Energy Conversion Storage* 2020;17(1).
- [25] Khan SS, Shareef H, Mutlag AH. Dynamic temperature model for proton exchange membrane fuel cell using online variations in load current and ambient temperature. *Int J Green Energy* 2019;16(5):361–70.
- [26] Spiegel C. PEM fuel cell modeling and simulation using MATLAB. Elsevier; 2011.
- [27] Lazarou S, Pyrgioti E, Alexandridis AT. A simple electric circuit model for proton exchange membrane fuel cells. *J Power Sources* 2009;190(2):380–6.
- [28] San Martín J, Zamora I, San Martín J, Aperribay V, Torres E, Eguia P. Influence of the rated power in the performance of different proton exchange membrane (PEM) fuel cells. *Energy* 2010;35(5):1898–907.
- [29] Razmjooy N, Ramezani M. Training wavelet neural networks using hybrid particle swarm optimization and gravitational search algorithm for system identification. *Int J Mechatronics, Electri Computer Tech* 2016;6(21):2987–97.
- [30] Yu D, Zhu H, Han W, Holburn D. Dynamic multi agent-based management and load frequency control of PV/Fuel cell/wind turbine/CHP in autonomous microgrid system. *Energy* 2019;173:554–68.
- [31] Fan X, Sun H, Yuan Z, Li Z, Shi R, Razmjooy N. Multi-objective optimization for the proper selection of the best heat pump technology in a fuel cell-heat pump micro-CHP system. *Energy Rep* 2020;6:325–35.



- [32] Gong W, razmjooy N. A new optimization algorithm based on OCM and PCM solution through energy reserve. *Int J Ambient Energy* 2020;1–47. no. just-accepted.
- [33] Tian M-W, Yan S-R, Han S-Z, Nojavan S, Jermstipparsert K, Razmjooy N. New optimal design for a hybrid solar chimney, solid oxide electrolysis and fuel cell based on improved deer hunting optimization algorithm. *J Clean Prod* 2020;249:119414.
- [34] Tizhoosh HR. Opposition-based learning: a new scheme for machine intelligence. In: *International conference on computational intelligence for modelling, control and automation and international conference on intelligent agents, web technologies and internet commerce (CIMCA-IAWTIC'06)*, vol. 1. IEEE; 2005. p. 695–701.
- [35] Çelik E. A powerful variant of symbiotic organisms search algorithm for global optimization. *Eng Appl Artif Intell* 2020;87:103294.
- [36] Rahnamayan S, Tizhoosh HR, Salama MM. Quasi-oppositional differential evolution. In: *2007 IEEE congress on evolutionary computation*. IEEE; 2007. p. 2229–36.
- [37] Yang D, Li G, Cheng G. On the efficiency of chaos optimization algorithms for global optimization. *Chaos, Solit Fractals* 2007;34(4):1366–75.
- [38] Rim C, Piao S, Li G, Pak U. A niching chaos optimization algorithm for multimodal optimization. *Soft Computing* 2018;22(2):621–33.
- [39] Arora S, Anand P. Chaotic grasshopper optimization algorithm for global optimization. *Neural Comput Appl* 2018:1–21.
- [40] Akkar HA, Mahdi FR. Grass fibrous Root optimization algorithm. *Int J Intell Syst Appl* 2017;11(6):15.
- [41] Wang G-G, Deb S, Cui Z. Monarch butterfly optimization. *Neural Comput Appl* 2019;31(7):1995–2014.
- [42] Ned Stack fuel cell technology. <http://www.fuelcellmarkets.com/content/images/articles/ps6.pdf>.
- [43] De Lira S, Puig V, Quevedo J. Robust lpv model-based sensor fault diagnosis and estimation for a pem fuel cell system. In: *2010 conference on control and fault-tolerant systems (SysTol)*. IEEE; 2010. p. 819–24.

